Carbohydrate Polymers 117 (2015) 657–665

Contents lists available at ScienceDirect

Carbohydrate Polymers

journal homepage: www.elsevier.com/locate/carbpol

Fabrication of porous zeolite/chitosan monoliths and their applications for drug release and metal ions adsorption

Yongli Zhang[a,b], Weiwei Yan[a,b], Zhiming Sun[a,b,*], Cheng Pan[c], Xue Mi[d,*], Gang Zhao[a,b], Jianping Gao[c,*]

[a] Huanhu Hospital, Tianjin 300060, PR China
[b] Tianjin Cerebral Vascular and Neural Degenerative Disease Key Laboratory, Tianjin 300060, PR China
[c] School of Science, Tianjin University, Tianjin 300072, PR China
[d] School of Medicine, Nankai University, Tianjin 300071, PR China

ARTICLE INFO

Article history:
Received 15 May 2014
Received in revised form 14 August 2014
Accepted 1 September 2014
Available online 19 September 2014

Keywords:
Zeolite
Chitosan
Porous material
Adsorption
Drug releasing

ABSTRACT

Ordered porous zeolite/chitosan (Zel/Chi) monoliths were prepared by a unidirectional freeze–drying method, and their properties and structures were characterized by various instrumental methods. The metal ion adsorption and the drug release performance of the porous Zel/Chi monoliths were also studied. The release rate of cefalexin from drug-loaded Zel/Chi monoliths depended on the composition and porous structure of the monoliths. The metal ion adsorption capacity of the Zel/Chi monoliths was related to the concentration of the metal ions, the adsorption time and the Zel/Chi ratio. An experimentally maximum adsorption of 89 mg/g was achieved for Cu^{2+} ions. The Zel/Chi monoliths with adsorbed Cu^{2+} ions effectively catalyzed the reduction of 4-nitrophenol to 4-aminophenol and had good recyclability. They were easily recovered by simply removing them from the reaction system and rinsing them with water.

1. Introduction

Porous materials are intriguing materials because of their unique characteristics and they have wide applications. Air and water pollution which include the presence of heavy metal ions are considered to be a serious health threat. So the treatment of heavy metal ion-containing wastewater has attracted much attention and several technologies have been developed for the removal of the heavy metal ions from industrial wastewater.

Chemical precipitation and oxidation–reduction methods transform soluble metal ions into insoluble compounds, but at the same time produce a great deal of waste sludge which can cause secondary pollution problems. Ion exchange resins can adsorb metal ions (Watanabe, Ohnaka, & Fujita, 2011), but they are expensive. Many porous materials have been used for the treatment of metal ion-containing water because they have high porosities and huge surface areas (Deze, Papageorgiou, Favva, & Katsaros, 2012; Zhang, Ma, &Yuan, 2008).

Zeolite is an important porous material. It has a uniform nanoporous structure that can selectively adsorb various pollutants like heavy metal ions and organic molecules (Meena, Mishra, & Rai, 2005). Zeolite 4A prepared from coal fly ash has been used to remove mixed heavy metal ions from water (Hui, Chao, & Kot, 2005). Cellulose acetate/zeolite (CA/Z) composite fibers have been synthesized and used as an adsorbent for removing Cu^{2+} and Ni^{2+} metal ions from aqueous solutions (Ji et al., 2012). The maximum theoretical adsorption capacities of the CA/Z fiber for Cu^{2+} and Ni^{2+} at 298 K were 28.57 and 16.95 mg/g, respectively.

Chitosan is a natural, non-toxic and biodegradable polymer. It has been used as a biomaterial in drug delivery systems and in scaffolds for tissue engineering. It also has high adsorbing efficiencies for organic molecules and metal ions which is because it contains various active functional groups such as amino and hydroxyl groups. These groups can chelate with metal ions. Recently chitosan based composites, like chitosan/bentonite (Futalan et al., 2011), chitosan/clinoptilolite (Dragan, Dinu, & Timpu, 2010), chitosan/fly ash composite (Wen, Tang, & Chen, 2011), chitosan/cellulose (Sun, Peng, Ji, Chen, & Li, 2009) and chitosan/cotton (Qu et al., 2009) have been prepared for removing metal ions from wastewater. Ethylenediamine modified chitosan had maximum adsorption capacities of 41.5, 31.8 and 20.0 for Cu^{2+}, Pb^{2+}, and Zn^{2+} ions, respectively (Chethan & Vishalakshi, 2013), and chitosan/sand exhibited

* Corresponding authors at: Tianjin University, School of Science, Tianjin 300072, PR China. Fax: +86 22 274 034 75.
E-mail addresses: szhm618@163.com (Z. Sun), tjumixue@163.com (X. Mi), jianpingg@eyou.com (J. Gao).

http://dx.doi.org/10.1016/j.carbpol.2014.09.018
0144-8617/

a capacity of 10.87 for Cu^{2+} ions (Wan Ngaha, Teong, & Hanafiah, 2011).

Composites made of chitosan and zeolite have been reported. The composites may be blends or chitosan coated zeolite (Ghosh, Ma, & Gao, 2013; Peng et al., 2013). They are usually in the forms of microspheres, particles, membranes, and films (Wan Ngaha, Teong, Toh, & Hanafiah, 2013; Batista, Villanueva, & Amorim, 2011). Zel/Chi beads and films has been used for metal ions adsorption, while the adsorption capacities are less than 52 mg/g (Wan Ngaha et al., 2013). Fabrication of porous Zel/Chi monoliths used for metal ion adsorption and drug release has not been reported.

At present, two main methods are used to prepare porous materials, porogenic and non-porogenic methods (Ishaug-Riley, Kruger, & Yaszemski, 1998; Yun & Jong, 2005). Freeze–drying is one of porogenic methods that is especially attractive because non-toxic water is usually used as the porogen to prepare the porous material (Stokols & Tuszynski, 2004). Recently, a unidirectional freeze–drying method (UFDM) was used to fabricate porous materials with oriented pore structures (Zhang, Long, & Cooper, 2005; Mi et al., 2012). To date, this is the simplest way to prepare oriented porous materials and the method has been exploited to prepare aligned porous inorganic, organic and composite materials.

Nacre is a strong inorganic material. Its toughness is due to its special architecture, where consists of a brick-and-mortar structure comprised of 95% (by vol) polycrystalline aragonite platelets and 5% of a protein that is extremely effective at restricting crack propagation (Bouville et al., 2014). Nacre has a strength that is orders of magnitude greater than either of its constituents. Its toughness is achieved through numerous extrinsic mechanisms including viscoelastic deformation of the protein layer, mineral bridge rupture, inelastic shearing and frictional sliding during platelet pull out. Various techniques, including UFDM have been used to produce strong inorganic/polymer composites that can mimic the features of nacre (Bouville et al., 2014).

Herein, highly porous zeolite/chitosan (Zel/Chi) monoliths were prepared by UFDM. The monoliths were then used to adsorb metal ions from aqueous solutions. The interconnected porous channels inside the porous monolith facilitated the diffusion of the ions, which benefited the adsorption. So the porous Zel/Chi monoliths showed a high adsorbing capacity. The Cu^{2+}-adsorbed monoliths demonstrated a high catalytic activity for the reduction of 4-nitrophenol to 4-aminophenol, and this material offers a promising way to remove heavy metal ions from wastewater.

2. Materials and methods

2.1. Materials

The zeolite was a gift from the Catalyst Plant at Nankai University, PR China. Chitosan (M_n = 100 K) was from Zhejiang Yuhuan Marine Biochemical Co. Ltd. Glutaraldehyde, the metal ion standard solutions, $NaBH_4$, 4-nitrophenol (4-NP), acetic acid, concentrated nitric acid, anhydrous ethanol and sodium hydroxide were all from Tianjin Chemical Reagent Co. All the chemicals were used as received.

2.2. Preparation of porous Zel/Chi monoliths

Chitosan powder (0.5 g) was dissolved with stirring in 50 mL of 0.2 mol/L acetic acid solution. Then the desired amount of zeolite powder and 1 mL of 5% (g/mL) glutaraldehyde solution (as the cross-linking agent) was added to the chitosan solution with sonication. The solution was allowed to age for about 2 h at room temperature, and then it was poured into a plastic tube. The plastic tube was then placed in an insulating Styrofoam container, with only the bottom surface of the plastic tube exposed. The Styrofoam container was placed onto the surface of a 6-cm diameter disk of metal, which in turn rested on a 6-cm-deep pool of liquid nitrogen to create a uniaxial thermal gradient. The solidified monoliths were then transferred into a freeze–drying vessel (Alpha1-2, Christ, German) under vacuum (less than 20 Pa) and freeze-dried for 48 h to give porous Zel/Chi monoliths.

The porous Zel/Chi monoliths were dipped in anhydrous ethanol containing a small amount of sodium hydroxide and slightly agitated. The monoliths were then removed and rinsed with pure anhydrous ethanol. The treated porous Zel/Chi monoliths were dried in the freeze drier for 6 h and stored in a drier. Similarly, drug-loaded porous Zel/Chi monoliths were prepared. Briefly, cefalexin was dissoved in distilled water, before it was added to Zel/Chi mixture solution under stir. The mixture solution was freeze dried to obtain the cefalexin loaded porous Zel/Chi monolith.

2.3. Observation of Zel/Chi monolith morphology

The morphology of porous Zel/Chi monoliths was observed by scanning electron microscope (SEM, JEOL-6700F ESEM, Japan). The samples were gold coated using a sputtering coater (Desk-II; Denton Vacuum), placed onto the stage in the chamber and observed.

2.4. Porosity of the porous Zel/Chi monoliths

The porosity of the porous Zel/Chi monoliths was calculated according to the following formula.

$$\text{Porosity}\ \ (\%) = \frac{V_m - V_p}{V_m} \times 100 = \frac{V_m - (W_m/\rho)}{V_m} \times 100 \qquad (1)$$

where V_m is the total volume of Zel/Chi monolith (cm^3), V_p is the actual volume taken by Zel/Chi (cm^3), W_m is the mass of the monoliths (g), and ρ is the density of Zel/Chi (g/cm^3). The ρ was obtained by measuring the weights (W) and volumes (V) of Zel/Chi composites discs ($\rho = W/V$).

2.5. Water absorption by the porous Zel/Chi monoliths

The Zel/Chi monoliths was placed into a vacuum at 50 °C and dried to a constant weight. They were then immersed into distilled water at room temperature. After 2 h, the samples were removed and their surface was blotted with filter paper before they were weighted. The water absorption (WA) of the Zel/Chi monoliths was calculated according to the following formula.

$$\text{WA}\ \ (\%) = \frac{W_t - W_0}{W_0} \times 100 \qquad (2)$$

where W_0 and W_t are the weights of Zel/Chi monoliths (g) before and after absorbing water, respectively.

2.6. Release of cefalexin from the Zel/Chi monoliths

The release of cefalexin was determined by placing the cefalexin-loaded Zel/Chi monolith (0.2 g) in 10 mL of saline solution at 37 °C. At certain time intervals, the saline solution was changed and the concentration of cefalexin in the eluate was determined using spectrophotometry. The accumulated amount of released cefalexin over time was calculated.

2.7. Adsorption capacity of the porous Zel/Chi monoliths for Cu^{2+} (or Pb^{2+})

The porous Zel/Chi monolith was put into a 100-mL conical flask containing 50 mL of 50 mg/L Cu^{2+} solution and allowed to

stand at room temperature. At 1 h intervals, 1 mL of the supernatant was removed and diluted to 50 mL with distilled water. Flame atomic absorption spectrophotometry (Soloar 969 atomic absorption spectrophotometer, Thermo, U.S.) was used to determine the concentration of the metal ion in the supernatant using a standard calibration curve. The adsorption efficiency (Ade) and saturated adsorption capacity (Q_s) were obtained using the following formula:

$$\text{Ade}\ (\%) = \frac{(C_0 - C_t)}{C_0} \times 100 \quad (3)$$

$$Q_t = \frac{(C_0 - C_t)V}{W} \quad (4)$$

where C_0 is the initial concentration of Cu^{2+} ions, C_t is the concentration at time t (h), W (g) is the weight of the porous Zel/Chi monolith, and V (mL) is the volume of solution. Q_t (mg/g) is the adsorption capacity of the porous monoliths at time t (h) and if the time is long enough it is equal to saturated adsorption capacity (Q).

2.8. Reduction of 4-NP catalyzed by Cu^{2+}-adsorbed Zel/Chi monoliths

The Cu^{2+}-adsorbed Zel/Chi monolith (30 mg) from the above experiment was rinsed three times with distilled water to remove any unbound Cu^{2+} and was then soaked in 0.5 M $NaBH_4$ solution (3 mL) for 19 min at 25 °C. Next an aqueous 4-NP solution of 0.015 M was added. The conversion of 4-NP to 4-AP was measured by monitoring the change in the 400-nm absorbance peak of 4-NP with a UV–vis spectrophotometer.

3. Results and discussion

3.1. Structure and properties of the porous Zel/Chi monoliths

The Zel/Chi monoliths were fabricated using different proportion of Zel/Chi via UDFM and their SEM photos are shown in Fig. 1. All the Zel/Chi monoliths contained randomly distributed pores although there are local areas where the pores are arranged regularly. The pores are all tube-like and parallelly arranged, so the cross-sectional (left) and vertical (right) images appear quite different. The layered structure of the Zel/Chi monoliths is similar to that of natural nacre but quite different from that of other porous materials prepared by traditional freeze–drying techniques. Those porous materials exhibit random and evenly distributed pores (Alizadeha, Abbasi, Khoshfetra, & Ghaleh, 2013), so their vertical and cross-sectional areas are nearly identical.

The shape of the pores in the Zel/Chi monoliths is due to the temperature gradient that occurred during the freezing step in the UFDM. When there is a temperature gradient during the phase separation, the ice crystals grow along the direction of the temperature gradient. The shape of the ice crystals then becomes imprinted in the porous monoliths during the freeze–drying, so the size and shapes of the pores in the Zel/Chi porous monoliths depend on the size and shapes of ice crystals.

The Zel/Chi ratio is an important factor that influences the structure of the Zel/Chi porous monoliths. Ratios of 1:1, 3:1, 5:1, 7:1, and 9:1 were used to prepare monoliths (the concentration of Chi was held constant). For all the Zel/Chi ratios, the size of the pores in the cross-sections are uneven; however, in the vertical-sections there is a layered structure and the distance between two layers corresponds to the width of the pores in cross-section. For the Zel/Chi ratio of 1:1, the width of the pores is 50 to 100 μm and the lengths are 300 to 600 μm (Fig. 1a and A). Both the width and length decreased when the Zel/Chi ratio increased. For a ratio of 7:1, the pore width decreased to about 30 μm and pore lengths decreased to 150 to 350 μm (Fig. 1d and D). This change is due to the increased amount of Zel at high Zel/Chi ratios. In the freezing step, a large amount of Zel (particles) prevents the ice from forming large ice crystals, so only small pores form in the Zel/Chi porous monoliths after the drying step.

Fig. 1F shows magnified SEM photos of the vertical section of the Zel/Chi porous monolith with a Zel/Chi ratio of 5:1. Both the Zel and Chi can be clearly seen. The Chi forms a continuous film and the Zel particles are surrounded by the Chi film or are adhered onto the film surface. At a high Zel content, so many Zel particles are on the film surface that the surface becomes coarse and the film thickness becomes thicker. When the Zel/Chi ratio was increased to 9:1 (Fig. 1e and E) it is difficult to see the porous structure, and the monolith is easily broken although it had high density. In addition, the film surface was much coarser and the Zel particles easily fell off the surface because there was not sufficient Chi to tightly glue the Zel particles together.

Fig. 2 shows the porosity of the Zel/Chi porous monoliths at different Zel/Chi ratios. The porosity increased almost linearly with decreasing Zel/Chi ratio. The Zel/Chi porous monolith with an 8:1 ratio only had a porosity of 68.8% whereas that for the 1:1 ratio was 96.9%. Hydroxyapatite (HA) and gelatin composite foams that have been previously formed via freeze–drying and crosslinking exhibited a similar porosity trend (Kim, Knowles, & Kim, 2005). Pure gelatin, gelatin-10% HA, and gelatin-30% HA had porosities of 89.8%, 87.5% and 84.6%, respectively.

Fig. 3 shows the IR spectra of Chi, Zel and Zel/Chi (7:1). The four absorption peaks at 1226.20, 1082.29, 800.45, and 545.40 cm^{-1} are due to Zel (Jansen, Van der Gaag, & Van Bekkum, 1984). The peaks at 1082.29 and 800.45 cm^{-1} are due to Si—O and Al—O stretching vibrations. CS has five peaks at 3441.57 cm^{-1} (—OH stretching), 2920.53 cm^{-1} (CH stretching), 1657.97 cm^{-1} (—NH_2 bending-I), 1571.20 cm^{-1} (—NH_2 bending-II), and 1081.72 cm^{-1} (C—O stretching) (Wang, Du, & Liu, 2004). The spectrum for Zel/Chi contains peaks for both Zel and Chi with some shifts in band positions. This indicates that there are some interactions between Zel and Chi but since no new peaks appeared in the Zel/Chi spectrum, no chemical reaction occurred between Zel and Chi.

Fig. 4 shows water absorption ability of the porous Zel/Chi monoliths made with different Zel/Chi ratios. As the relative amount of Chi in the Zel/Chi increased, the water adsorption ability also increased. This same trend was also observed for HA/gelatin composite foams (Kim et al., 2005). As the amount of HA increased, the water absorption of the HA/gelatin foams decreased from 1010% to 751%. This was attributed to the decrease in the porosity and the more compact structure of the higher HA-content foams and to the lower water absorption ability of HA powder compared to gelatin.

It has been reported that Zeolite A microspheres with particle sizes of ~700 μm only absorb about 290 mg of water per g of absorbent (Liang, Jie, & Zeng, 2012). The high water adsorption of the Zel/Chi monoliths in Fig. 4 is due to their high porosities and the high water uptake ability of chitosan. The ordered structure of the monoliths combined with their high water adsorption abilities should make it convenient for the diffusion of molecules or ions, which is beneficial for chemical reactions and the adsorption of metal ions.

3.1.1. Drug release in vitro from the porous Zel/Chi monoliths

The release profiles of cefalexin from the Zel/Chi monoliths are shown in Fig. 5. For all the Zel/Chi monoliths, the release of cefalexin is rapid at the beginning, then it slows and finally reaches a constant. Fig. 5A shows that the total release percentage of cefalexin from the Zel/Chi monoliths decreased as the concentration of Zel/Chi solution used to prepare the porous monoliths increased. A high concentration of Zel/Chi, the drug is deeply covered by the materials, so the release rate is reduced.

The release patterns of the Zel/Chi monoliths prepared from different Zel/Chi ratios were also investigated (Fig. 5B). When the relative content of Zel in Zel/Chi was increased the cefalexin release rate accelerated, but the cumulative release decreased. The Zel/Chi monoliths with high Chi content have a high water uptake ability, so their corresponding cefalexin releasing rate should be higher than the Zel/Chi monoliths with lower Chi content. However, the experimental results are just the opposite. The Chi may seal the Zel nanopores and block the diffusion of the cefalexin molecules through the monolith. So the porous Zel/Chi monolith with a higher Chi content has a lower releasing rate. However, a low Zel content resulted in weak cephalexin adsorption and in the end the material has a high cumulative release.

The release patterns of cefalexin from the Zel/Chi monoliths in solutions with different pH values are showed in Fig. S1. As shown in Fig. S1, cefalexin release in pH 2. was faster than those in pH 4.5 and 6.5. At low pH, the NH_3 groups become protonated to NH_3^+. The electron positive groups repel each other, resulting in high swelling

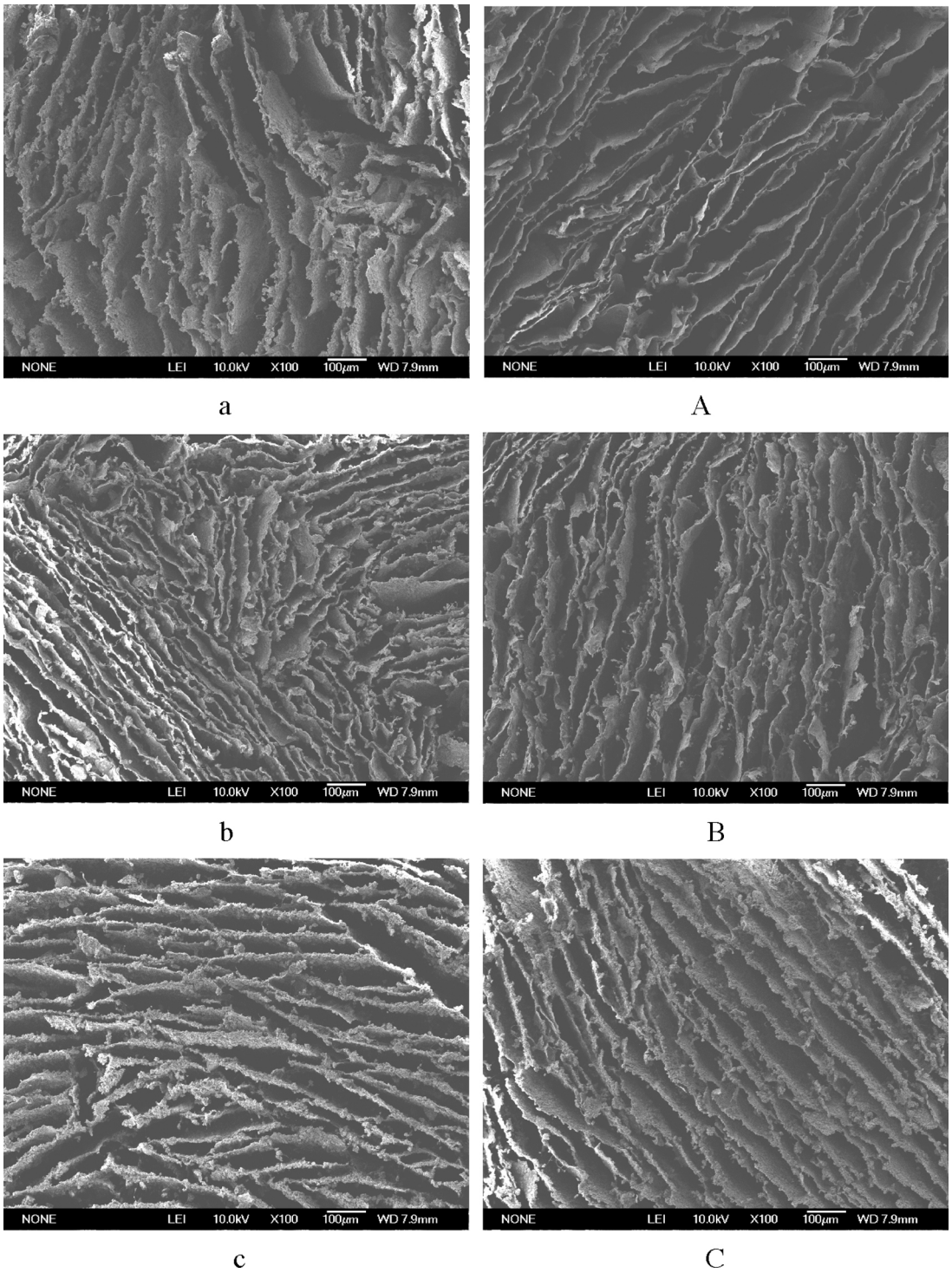

Fig. 1. The SEM images of porous Zel/Chi monoliths made from different proportions of Zel/Chi; cross-sections ((a)–(e)) and vertical sections ((A)–(E)). F is the magnified photos of C. Zel/Chi ratio: ((a) and (A) 1:1, ((b) and (B)) 3:1, ((c) and (C)) 5:1, ((d) (D)) 7:1, ((e) and (E)) 9:1.

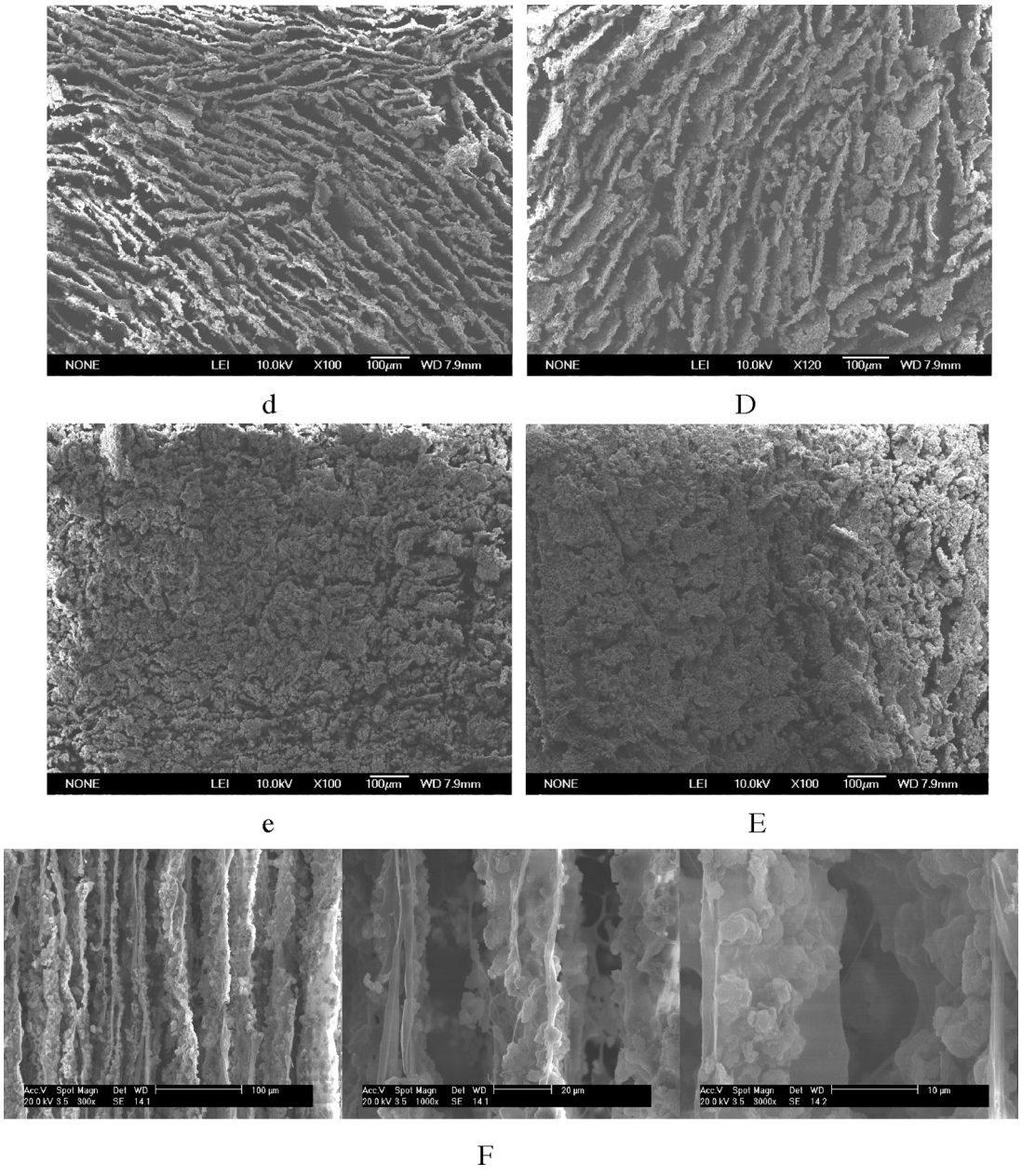

Fig. 1. (*Continued*).

of Zel/Chi monoliths in acid medium compared with their swelling in neutral medium. So the dissolution and diffusion of drug are fast in low pH. Similar phenomenon was also found in matrix tablets made of chitosan and triptolide (Huanbutt, Cheewatanakornkool, Terada, Nunthanid, & Sriamornsak, 2013).

Zeolite has been used as a carrier for the controlled release of drugs. Guo et al. compared the release processes of gentamicin in Gent-ZSM-5 and Gent-HAPs (Guo, Long, Song, & Zhu, 2014). They found that the Gent-HAPs initially displayed a burst-release with more than 90% of the loaded gentamicin released in the first 6 h. In contrast Gent-ZSM-5 exhibited a slow and sustained release of gentamicin. The effective drug release time was more than 6 days (60.2%), which is close to the time needed for prophylactic use of antibiotics in postoperative treatment. Zhai (2012) investigated the release of cefalexin from the pores of SBA-15. Cefalexin was quickly released within 1–5 h and the cumulative release reached 50% at 5 h. After 15–20 h, the sustained release speed of cefalexin decreased.

Sustained and controlled release of gentamicin from chitosan films has been studied for application as a wound dressing film (Campos, Rawls, Innocentini-Mei, & Satsangi, 2009). It was found that the gentamicin cumulative release changed from 18% to 67% at 14 days and was dependent on the degree of chitosan crosslinking and the initial gentamicin concentration. Gentamicin loaded PCL (poly(e-caprolactone)) scaffolds have also been fabricated by a freeze drying method (Sezer, Arslantunali, Aksoy, Hasirci, & Hasirci, 2014). The total drug-release amounts were found to be approximately 67%, 74%, and 87% of the total loaded drug content after 216 h for PCL-10β/G (10 wt% gentamicin-loaded-TCP–gelatin microsphere), PCL-30β/G, and PCL-50β/G, respectively. The release rate of cefalexin from the Zel/Chi monoliths is obviously higher than that of gentamicin from the chitosan films. The unidirectional porous structure of the Zel/Chi monoliths may be the reason for the high release rate of cefalexin. In addition, if the Zel/Chi monoliths are used as implants, ordered porous structure is important for the cell culture, exchanging nutrients and

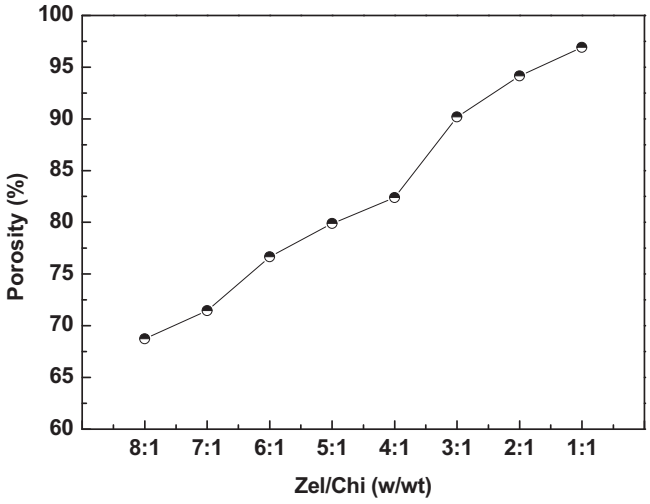

Fig. 2. Porosity of the Zel/Chi porous monoliths with different Zel/Chi ratios.

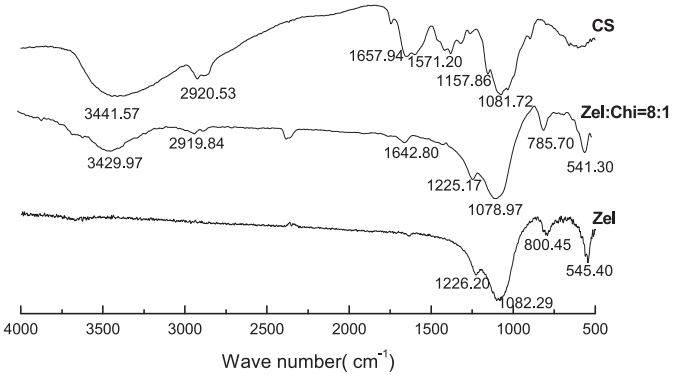

Fig. 3. IR spectra of Zel, CS and Zel/Chi (7:1).

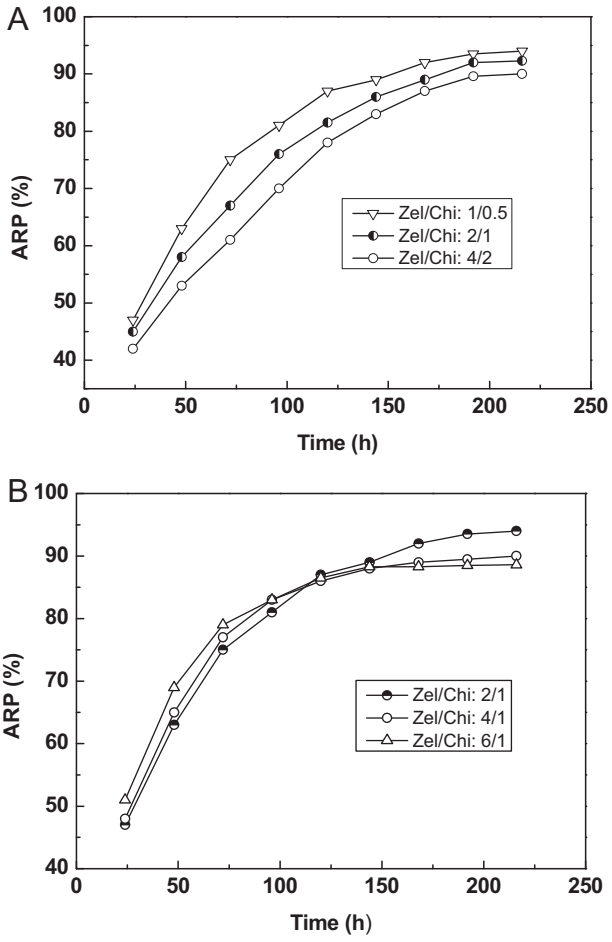

Fig. 5. Accumulated cefalexin released from the porous Zel/Chi monoliths with different Zel/Chi concentrations (A) and prepared from different Zel/Chi ratios (B).

metabolized cell products, as well as diffusion of metal ions for adsorption.

Hemorrhaging is still a leading cause of death after trauma, especially for those with infectious complications. Treatment with hemostatic materials is a common way to deal with bleeding. Some hemostatics have been developed to arrest massive bleeding, such as HemCon (a chitosan dressing) and QuikClot (a zeolite powder) both of which are routinely used on battlefields because of their efficiency in reducing or stopping bleeding (Wedmore, McManus, Pusateri, & Holcomb, 2006; Rhee et al., 2008; Ward et al., 2007).

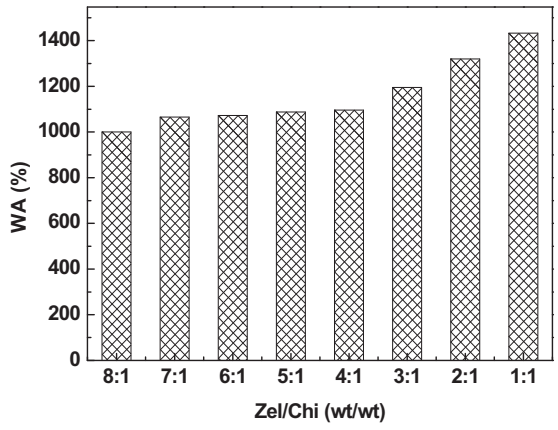

Fig. 4. Water adsorption of porous Zel/Chi monoliths made with different Zel/Chi ratios.

Zeolite is biocompatible and has a uniform nanoporous structure that absorbs water. When applied to a bleeding surface, it can quickly absorb water molecules from the blood and facilitate the formation of a crust layer of platelets and blood proteins and, thus, stops the bleeding. A chitosan dressing can adhere to a wound on contact with blood, and attracts red blood cells to form a clot after a certain time. Cefalexin loaded porous Zel/Chi monoliths could not only make full use of the above characteristics of chitosan and

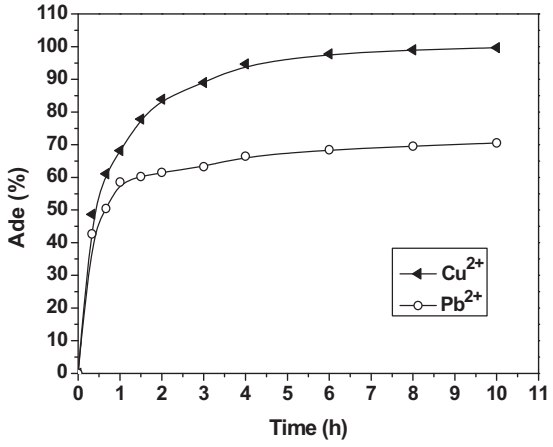

Fig. 6. Adsorption of metal ions by the porous Zel/Chi monoliths concentration of metal ions: 50 mg/L, Zel/Chi = 1:1.

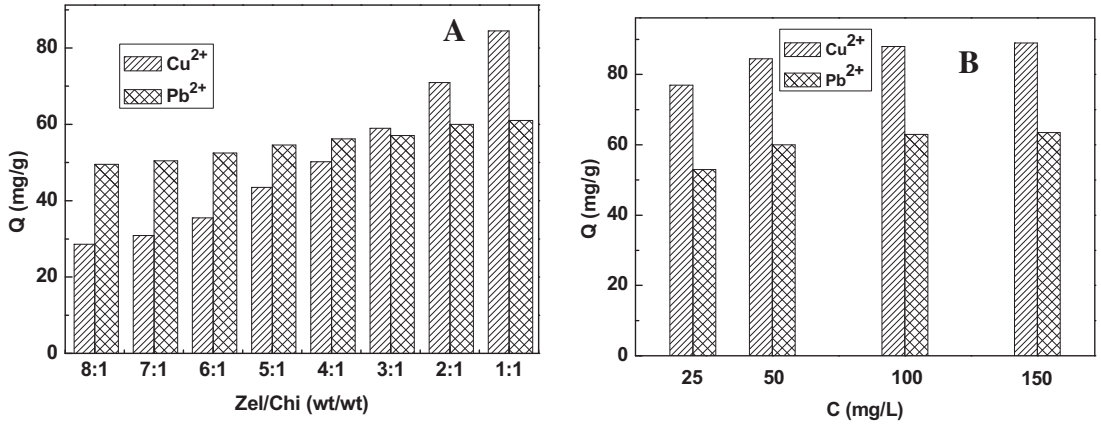

Fig. 7. Adsorption of Cu^{2+} and Pb^{2+} ions by the Zel/Chi porous monoliths prepared with different Zel/Chi ratios (A) and in different metal ion concentrations (B).

zeolite to create a potential hemostatic material like QuikClot and HemCon, but could also reduce infections. In addition, the water uptake results indicate that the Zel/Chi monoliths should have a huge adsorption capacity for blood, which will be studied in the future.

3.1.2. Adsorption of metal ions by the porous Zel/Chi monoliths

Porous materials are often used to adsorb metal ions because they have large surface areas. Heavy metal exposure is a growing health problem worldwide. Various commercial naturopathic and homeopathic remedies are used to remove harmful metals from people that have been exposed to heavy metals such as *N*-acetylcysteine, glutathione, selenocysteine, zinc, charcoal, zeolite, EDTA, and alginate. Sangvanich et al. (2014) developed an oral treatment for heavy metal poisoning based on thiol-modified nanoporous silica. It has a very high affinity for Pb^{2+} and Cd^{2+} and is superior to sorbents with carboxylic acid or phosphonic acid ligands and to commercially available metal chelating sorbents.

The ability of the Zel/Chi porous monoliths (Zel/Chi = 1:2) to adsorb Cu^{2+} and Pb^{2+} ions over time was investigated and the results are shown in Fig. 6. The adsorption efficiency increased rapidly initially and then the adsorption rate slowed and finally reached a maximum. The time to reach the maximum for the Pb^{2+} ions was shorter than that for the Cu^{2+} ions, but the adsorption maximum for Pb^{2+} was lower than that for Cu^{2+}.

Fig. 7A shows the adsorption of Cu^{2+} and Pb^{2+} ions by the Zel/Chi monoliths prepared with different Zel/Chi ratios. The adsorption capacity for Cu^{2+} ions increased as the Zel/Chi ratio decreased. The adsorption capacity for Pb^{2+} ions also increased with decreasing Zel/Chi ratio but more slowly. The adsorption maxima were 85 and 60 mg/g for Cu^{2+} and Pb^{2+}, respectively. Zeolite 4A prepared from coal fly ash has been reported to remove heavy metal ions in wastewater with a maximum adsorption capacity of 40.1 mg/g for Cu^{2+} ions (Hui et al., 2005). A maximum adsorption capacity of 0.207 mmol/g (42.8 mg/g) for Pb^{2+} by natural Mongolian zeolite has also been reported (Batjargal, Yang, Kim, & Baek, 2011).

The effect of the initial concentration of metal ion (20, 50, 100 and 150 mg/L) on the adsorption ability of the porous Zel/Chi monoliths (Zel/Chi = 1:1) was also investigated and the results are shown in Fig. 7B. For both Pb^{2+} and Cu^{2+}, the adsorption capacity of the Zel/Chi monoliths increased when the metal ions concentration increased. This is the normal trend for the adsorption of metal ions or organics by adsorbents. At high metal ion concentrations, more ions are adsorbed by the Zel/Chi monoliths, resulting in an increase in the adsorption capacity. However, the growth trend will stop due to saturation effects when the initial concentration of metal ions increases to a certain value.

Fig. S2a shows the adsorption of Cu^{2+} and Pb^{2+} ions by the Zel/Chi monoliths at different pH values. The effect of pH is obvious and the similar results were also reported (Hasan, Ghosh, Viswanath, & Boddu, 2008; Laus, Costa, Szpoganicz, & Favere, 2010). The *Q* increased as the pH increased and reached a maximum at pH 6. At lower pH values, the H^+ ions in solution compete with Cu^{2+} (Pb^{2+}) for adsorption, which leads to reduced Cu^{2+}

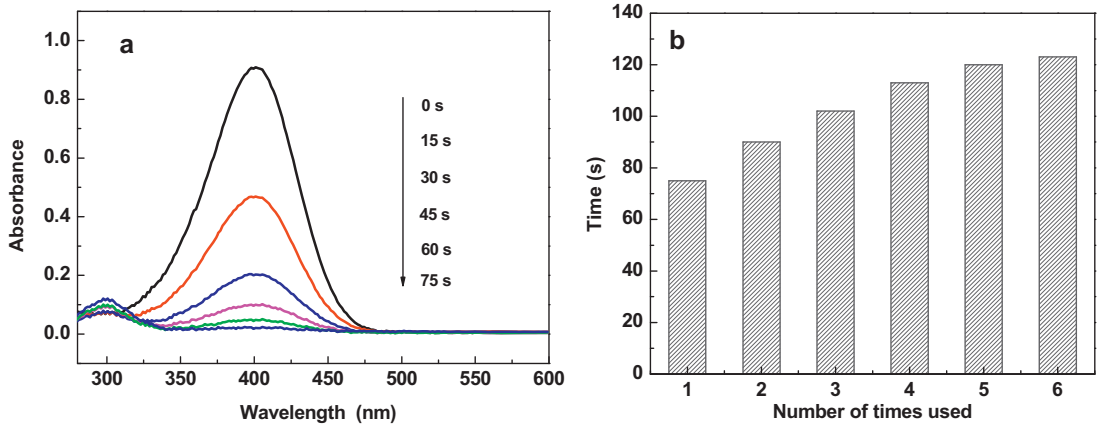

Fig. 8. UV–vis absorption spectra for the reduction of 4-NP by $NaBH_4$ in the presence of Cu@Zel/Chi (a) and recyclability of Cu@Zel/Chi (b).

adsorption. In addition, at low pH, the NH_3 groups become protonated to NH_3^+. These NH_3^+ cations not only do not chelate with Cu^{2+}, but also induce electrostatic repulsions with the Cu^{2+} ions in solution. This prevents the Cu^{2+} ions from approaching to and coordination with the Chi macromolecules. When the pH was above 7.0, $Cu(OH)_2$ formed. The results in Fig. S2b demonstrates that the effect of temperature on the Q is unobvious.

Cellulose acetate/zeolite (CA/Z) composite fibers have been used as an adsorbent for removing Cu^{2+} and Ni^{2+} metal ions from aqueous solutions (Ji et al., 2012). The maximum theoretical adsorption capacity of the CA/Z fibers for Cu^{2+} was 28.57 mg/g. Zel/Chi beads showed adsorption capacities of less than 52 mg/g for Cu^{2+} ions (Wan Ngaha et al., 2013), which is lower than that of the Zel/Chi monoliths. The high metal ions adsorption by Zel/Chi monoliths is attributed to the ordered porous structure. The above results indicate that the porous Zel/Chi monoliths have a high adsorption capacity for metal ions. So they may be useful for oral treatment for heavy metal poisoning if they are molded to porous microspheres.

Nitrophenolic compounds are the most common organic pollutant in agricultural and industrial waste waters, and it is necessary to establish methods to convert 4-NP to 4-AP under mild conditions. Here, the Zel/Chi monoliths with adsorbed Cu^{2+} ions (Cu@Zel/Chi) were used to catalyze the reduction of 4-NP to 4-AP. When the reduction of 4-NP started, the absorption intensity at 400 nm gradually decreased with a concurrent increase in a new absorption peak at 300 nm. This is due to the formation of 4-AP. So UV–vis absorption spectra provide an easy way to trace the reduction process.

As shown in Fig. 8a, after the Cu@Zel/Chi was added to the reactants, the absorption intensity at 400 nm decreased rapidly with time, and the reduction reaction was complete in about 75 s. The calculated rate constant (K) is $6.38 \times 10^{-2}\ s^{-1}$ which is a fast reaction rate compared with those of other Cu-based catalysts. For example Cu nanoparticles encapsulated in 4G PAMAM-OH dendrimers have a K value of $2.43 \times 10^{-2}\ s^{-1}$ (Nemanashi & Meijboom, 2013). Cu nanoparticles inside poly(2-acrylamido-2-methyl-1-propansulfonic acid) hydrogel networks were used in the reduction of 4-nitrophenol and had a K value of $1.72 \times 10^{-3}\ s^{-1}$(Sahiner & Ozay, 2012). The high reaction rate for the Cu@Zel/Chi is probably due to good diffusion of the reactants through the porous catalyst system.

The recyclability of the Cu@Zel/Chi was also tested and as the results in Fig. 8b show, the Cu@Zel/Chi was successfully reused for six successive cycles and the reaction was still complete within 2 min. Thus the Cu@Zel/Chi monoliths show good catalytic activity and recyclability. So Zel/Chi monoliths can effectively adsorb Cu^{2+} ions which can then be used to turn a toxic waste material into a useful catalyst.

4. Conclusions

Ordered porous zeolite/chitosan (Zel/Chi) monoliths and cephalexin-loaded Zel/Chi monoliths were prepared by a unidirectional freeze–drying method. The release rates of the cefalexin-loaded Zel/Chi monoliths depended on the composition and porous structure of the monoliths. The adsorption capacity of the Zel/Chi monoliths for metal ions depended on the adsorbing time, the Zel/Chi ratio and the metal ion concentration. For Cu^{2+}, the maximum adsorption was 89 mg/g. The Zel/Chi monoliths with adsorbed Cu^{2+} ions efficiently catalyzed the reduction of 4-nitrophenol to 4-aminophenol. The porous monoliths are biocompatible and reusable, which means they could be used as scaffolds in tissue engineering and as sorbents to remove heavy metal ions from body of people and water.

Appendix A. Supplementary data

Supplementary data associated with this article can be found, in the online version, at http://dx.doi.org/10.1016/j.carbpol.2014.09.018.

References

Alizadeha, M., Abbasi, F., Khoshfetra, A. B., & Ghaleh, H. (2013). Microstructure and characteristic properties of gelatin/chitosan scaffold prepared by a combined freeze–drying/leaching method. *Materials Science and Engineering C*, *33*, 3958–3967.

Batista, A. C. L., Villanueva, E. R., & Amorim, R. V. S. (2011). Chromium (VI) Ion adsorption features of chitosan film and Its chitosan/zeolite conjugate 13× film. *Molecules*, *16*, 3569–3579.

Batjargal, T., Yang, J. S., Kim, D. H., & Baek, K. (2011). Removal characteristics of Cd(II), Cu(II), Pb(II), and Zn(II) by natural mongolian zeolite through batch and column experiments. *Separation Science and Technology*, *46*, 1313–1320.

Bouville, F., Maire, E., Meille, S., Van de Moortèle, B., Stevenson, A. J., & Deville, S. (2014). Strong, tough and stiff bioinspired ceramics from brittle constituents. *Nature Materials*, *13*, 508–514.

Campos, M. G. N., Rawls, H. R., Innocentini-Mei, L. H., & Satsangi, N. (2009). In vitro gentamicin sustained and controlled release from chitosan cross-linked films. *Journal of Materials Science Materials in Medicine*, *20*, 537–542.

Chethan, P. D., & Vishalakshi, B. (2013). Synthesis of ethylenediamine modified chitosan and evaluation for removal of divalent metal ions. *Carbohydrate Polymers*, *97*, 530–536.

Deze, E. G., Papageorgiou, S. K., Favva, E. P., & Katsaros, F. K. (2012). Porous alginate aerogel beads for effective and rapid heavy metal sorption from aqueous solutions: effect of porosity in Cu^{2+} and Cd^{2+} ion sorption. *Chemical Engineering Journal*, *209*, 537–546.

Dragan, E. S., Dinu, M. V., & Timpu, D. (2010). Preparation and characterization of novel composites based on chitosan and clinoptilolite with enhanced adsorption properties for Cu^{2+}. *Bioresource Technology*, *101*, 812–817.

Futalan, C. M., Kan, C. C., Dalida, M. L., Hsien, K. J., Pascua, C., & Wan, M. W. (2011). Comparative and competitive adsorption of copper, lead, and nickel using chitosan immobilized on bentonite. *Carbohydrate Polymers*, *83*, 528–536.

Ghosh, A., Ma, L., & Gao, C. Y. (2013). Zeolite molecular sieve 5A acts as a reinforcing filler, altering the morphological, mechanical, and thermal properties of chitosan. *Journal of Materials Science*, *48*, 3926–3935.

Guo, Y. P., Long, T. Z., Song, F., & Zhu, Z. A. (2014). Hydrothermal fabrication of ZSM-5 zeolites: Biocompatibility, drug delivery property, and bactericidal property. *Journal of Biomedical Materials Research*, *102B*, 583–591.

Hasan, S., Ghosh, T. K., Viswanath, D. S., & Boddu, V. M. (2008). Dispersion of chitosan on perlite for enhancement of copper(II) adsorption capacity. *Journal of Hazardous Materials*, *152*, 826–837.

Hui, K. S., Chao, C. Y. H., & Kot, S. C. (2005). Removal of mixed heavy metal ions in wastewater by zeolite 4A and residual products from recycled coal fly ash. *Journal of Hazardous Materials*, *127*, 89–101.

Huanbutt, K., Cheewatanakornkool, K., Terada, K., Nunthanid, J., & Sriamornsak, P. (2013). Impact of salt form and molecular weight of chitosan on swelling and drug release from chitosan matrix tablets. *Carbohydrate Polymers*, *97*, 26–33.

Ishaug-Riley, S. L., Kruger, G. M., & Yaszemski, M. J. (1998). Three-dimensional culture of ratcalvarial osteoblasts in porous biodegradable polymers. *Biomaterials*, *19*, 1405–1412.

Jansen, J. C., Van der Gaag, F. J., & Van Bekkum, H. (1984). Identification of ZSM-type and other 5-ring containing zeolites by IR spectroscopy. *Zeolites*, *4*, 369–372.

Ji, F., Li, C. L., Tang, B., Xu, J. H., Lu, G., & Liu, P. (2012). Preparation of cellulose acetate/zeolite composite fiber and its adsorption behavior for heavy metal ions in aqueous solution. *Chemical Engineering Journal*, *209*, 325–333.

Kim, H. W., Knowles, J. C., & Kim, H. (2005). Hydroxyapatite and gelatin composite foams processed via novel freeze–drying and crosslinking for use as temporary hard tissue scaffolds. *Journal of Biomedical Materials Research*, *72A*, 136–145.

Laus, R., Costa, T. G., Szpoganicz, B., & Favere, V. T. (2010). Adsorption and desorption of Cu(II), Cd(II) and Pb(II) ions using chitosan crosslinked with epichlorohydrin–triphosphate as the adsorbent. *Journal of Hazardous Materials*, *183*, 233–241.

Liang, Y., Jie, G., & Zeng, C. F. (2012). Synthesis of monodisperse zeolite A/chitosan hybrid microspheres and binderless zeolite A microspheres. *Industrial & Engineering Chemistry Research*, *51*, 2299–2308.

Meena, A. K., Mishra, G. K., & Rai, P. K. (2005). Removal of heavy metal ions from aqueous solutions using carbon aerogel as an adsorbent. *Journal of Hazardous Materials*, *122*, 161–170.

Mi, X., Gao, J. P., Wang, X. D., Xu, F. Q., Xin, F. B., Wen, P., et al. (2012). Fabrication of highly porous starch monoliths and their application as green desiccants. *Polymers for Advanced Technologies*, *23*, 38–44.

Nemanashi, M., & Meijboom, R. (2013). Synthesis and characterization of Cu, Ag and Au dendrimer-encapsulated nanoparticles and their application in the reduction of 4-nitrophenol to 4-aminophenol. *Journal of Colloid and Interface Science*, *389*, 260–267.

Peng, S., Zeng, Q. H., Guo, Y. H., Niu, B. B., Zhang, X., & Hong, S. (2013). Defluoridation from aqueous solution by chitosan modified natural zeolite. *Journal of Chemical Technology and Biotechnology*, *88*, 1707–1714.

Qu, R., Sun, C., Ma, F., Zhang, Y., Ji, C., Xu, Q., et al. (2009). Removal and recovery of Hg(II) from aqueous solution using chitosan-coated cotton fibers. *Journal of Hazardous Materials*, *167*, 717–727.

Rhee, P., Brown, C., Martin, M., Salim, A., Plurad, D., Green, D., et al. (2008). QuikClot use in trauma for hemorrhage control: case series of 103 documented uses. *Journal of Trauma*, *64*, 1093–1099.

Sahiner, N., & Ozay, O. (2012). Enhanced catalytic activity in the reduction of 4-nitrophenol and 2-nitrophenol by p(AMPS)-Cu (0) hydrogel composite materials. *Current Nanoscience*, *8*, 357–374.

Sangvanich, T., Morry, J., Fox, C., Ngamcherdtrakul, W., Goodyear, S., David, C., et al. (2014). Novel oral detoxification of mercury, cadmium, and lead with thiol-modified nanoporous silica. *ACS Applied Materials & Interfaces*, *6*, 5483–5493.

Sezer, U. A., Arslantunali, D., Aksoy, E. A., Hasirci, V., & Hasirci, N. (2014). Poly(e-caprolactone) composite scaffolds loaded with gentamicin-containing *b*-tricalcium phosphate/gelatin microspheres for bone tissue engineering applications. *Journal of Applied Polymer Science*, *131* http://dx.doi.org/10.1002/APP.40110

Stokols, S., & Tuszynski, M. H. (2004). The fabrication and characterization of linearly oriented nerve guidance scaffolds for spinal cord injury. *Biomaterials*, *25*, 5839–5846.

Sun, X., Peng, B., Ji, Y., Chen, J., & Li, D. (2009). Chitosan(chitin)/cellulose composite biosorbents prepared using ionic liquid for heavy metal ions adsorption. *AIChE Journal*, *55*, 2062–2069.

Wan Ngaha, W. S., Teong, L. C., & Hanafiah, M. A. K. M. (2011). Adsorption of dyes and heavy metal ions by chitosan composites: A review. *Carbohydrate Polymers*, *83*, 1446–1456.

Wan Ngaha, W. S., Teong, L. C., Toh, R. H., & Hanafiah, M. A. K. M. (2013). Comparative study on adsorption and desorption of Cu(II) ions by three types of chitosan–zeolite composites. *Chemical Engineering Journal*, *223*, 231–238.

Wang, X. H., Du, Y. M., & Liu, H. (2004). Preparation, characterization and antimicrobial activity of chitosan–Zn complex. *Carbohydrate Polymers*, *56*, 21–26.

Ward, K. R., Tiba, M. H., Holbert, W. H., Blocher, C. R., Draucker, G. T., Proffitt, E. K., et al. (2007). Comparison of a new hemostatic agent to current combat hemostatic agents in a swine model of lethal extremity arterial hemorrhage. *Journal of Trauma*, *63*, 276–284.

Watanabe, Y., Ohnaka, K., & Fujita, S. (2011). Effects of the spaces available for cations in strongly acidic cation-exchange resins on the exchange equilibria by quaternary ammonium ions and on the hydration states of metal ions. *Analytical Chemistry*, *83*, 7480–7485.

Wedmore, I., McManus, J., Pusateri, A. E., & Holcomb, J. B. (2006). A Special report on the chitosan-based hemostatic dressing: experience in current combat operations. *Journal of Trauma*, *60*, 655–658.

Wen, Y., Tang, Z., Chen, Y., & Gu, Y. (2011). Adsorption of Cr(VI) from aqueous solutions using chitosan-coated fly ash composite as biosorbent. *Chemical Engineering Journal*, *175*, 110–116.

Yun, H. L., & Jong, H. L. (2005). Electrospun dual-porosity structure and biodegradation morphology of montmorillonite reinforced PLLA nanocomposite scaffolds. *Biomaterials*, *26*, 3165–3172.

Zhai, Q. Z. (2012). Inclusion of cefalexin in SBA-15 mesoporus material and release property. *Materials Science and Engineering C*, *32*, 2411–2417.

Zhang, H., Long, J., & Cooper, A. I. J. (2005). Aligned porous materials by directional freezing of solutions in liquid CO_2. *Journal of the American Chemical Society*, *127*, 13482–13483.

Zhang, X. J., Ma, T. Y., & Yuan, Z. Y. (2008). Titania–phosphonate hybrid porous materials: preparation, photocatalytic activity and heavy metal ion adsorption. *Journal of Materials Chemistry*, *18*, 2003–2010.